Quasiperiodic Pb monolayer on the fivefold *i*-Al-Pd-Mn surface: Structure and electronic properties

M. Krajčí,[1,2,*] J. Hafner,[2] J. Ledieu,[3] V. Fournée,[3] and R. McGrath[4]
[1]*Institute of Physics, Slovak Academy of Sciences, Dúbravská cesta 9, SK-84511 Bratislava, Slovak Republic*
[2]*Fakultät für Physik and Center for Computational Materials Science, Universität Wien, Sensengasse 8/12, A-1090 Wien, Austria*
[3]*Institut Jean Lamour, UMR 7198 CNRS, Nancy-Université-UPVM, Ecole des Mines, Parc de Saurupt, 54042 Nancy Cedex, France*
[4]*Surface Science Research Centre and Department of Physics, The University of Liverpool, Liverpool L69 3BX, United Kingdom*
(Received 11 May 2010; revised manuscript received 22 July 2010; published 11 August 2010)

Lead is one of few elements that adopts a pseudomorphic structure when deposited on quasicrystalline substrates. We present a structural model of quasiperiodic Pb overlayers formed on the fivefold surface of an icosahedral Al-Pd-Mn quasicrystal at two different coverages close to saturation. The skeleton of the Pb monolayer is formed by a network of "starfish" (SF) clusters formed at the initial stages of Pb deposition, as studied in detail in our previous work [Ledieu *et al.*, Phys. Rev. B **79**, 165430 (2009)]. The atomic structure of the Pb monolayers can be represented as a decorated pentagonal Penrose P1 tiling. The structural models reproduce also the quasiperiodic superstructure of the layers observed in experimental scanning tunneling microscopy (STM) images which is described by the τ-scaled τP1 tiling (τ is the golden mean). The atomic structure underlying the observed τ-scaled "white flower" motifs and the origin of irregular bright spots in STM images are discussed. The bright spots appear in the centers of the SF clusters centered at substrate sites occupied by Al atoms. The calculated electronic structure shows that the minimum in the density of states (pseudogap) at the Fermi level which is characteristic for the Al-Pd-Mn quasicrystals appears also in the local density of states of the adsorbed Pb monolayer. However, our analysis demonstrates that the formation of this pseudogap is not due to the quasiperiodic arrangement of the Pb atoms but to the strong hybridization of their orbitals with the substrate.

DOI: 10.1103/PhysRevB.82.085417 PACS number(s): 61.44.Br, 68.35.bd, 68.37.Ef, 71.23.Ft

I. INTRODUCTION

Adsorbates on quasicrystalline surfaces can potentially create novel forms of matter with interesting physicochemical properties. While the surfaces of ordinary crystals provide only a few inequivalent sites for the adsorption of atoms or molecules, the complex landscape of a quasicrystalline surface provides a rich variety of adsorption sites. During recent years many attempts have been made to produce quasiperiodic single-element overlayers on quasicrystalline substrates.[1–16] It is known that in the bulk quasicrystalline ordering is realized only in multicomponent alloys and therefore the possibility to produce quasiperiodic single-element overlayers is of fundamental importance. However, to grow a thin film with quasiperiodic long-range order turned out to be rather difficult. Most of attempts to fabricate quasicrystalline single-element films resulted in amorphous or polycrystalline films with domains of common crystalline structures.[1–3,5,6] Lead is one of few elements that adopts a pseudomorphic structure when deposited on quasicrystalline substrates[14,16] and therefore it deserves particular attention. In our recent work[14] a quasiperiodic Pb monolayer on the fivefold *i*-Al-Pd-Mn surface has been successfully prepared and characterized using scanning tunneling microscopy (STM) and other experimental techniques. The nucleation of small Pb clusters on the fivefold Al-Pd-Mn surface during the early stages of the deposition has been investigated both experimentally and by *ab initio* calculations.[16] It was found that nucleation proceeds via the formation of pentagonal islands nicknamed "starfish" (SF) clusters. The atomic structure of these clusters has been resolved and the calculations confirmed their structural stability. In this work, we go a step further and investigate the structure and electronic properties of the whole monolayer.

In our previous *ab initio* density-functional studies,[17–19] we have explored the conditions for the formation of quasiperiodic overlayers on a fivefold surface of an icosahedral Al-Pd-Mn quasicrystal. In Ref. 17 we have investigated formation of dense Sn, Bi, and Sb adlayers. We have found that on the fivefold surface of *i*-Al-Pd-Mn, Bi, Sn, and Sb atoms preferentially occupy the vertices of a quasiperiodic tiling, forming the skeleton of a quasiperiodic ordering. However, the remaining atoms decorating the interior of the tiles are arranged more irregularly, possibly because of a conflict between the interactions among the atoms forming the layer and their binding to the substrate. On the other hand, we predicted that highly regular quasiperiodic monolayers can be formed by Na and K atoms on the fivefold surface of *i*-Al-Pd-Mn surface,[18] and this was later confirmed experimentally.[15] Structurally stable quasiperiodic monolayers can be formed on quasiperiodic substrates only. Unsupported quasiperiodic monolayers are unstable.[17] The atomic arrangement in a quasiperiodic adlayer is the result of a complex interplay between the structure of the substrate, the adatom/substrate interactions, and the lateral interaction between adatoms in the adlayer. Understanding the structure of the substrate is therefore a prerequisite for understanding the structure of the adlayer. The structure of the clean fivefold Al-Pd-Mn surface is now well understood: the theoretical model[20,21] derived from the Katz-Gratias-Boudard (KGB) model of the bulk quasicrystal is in good agreement with experiment. STM studies with atomic resolution have iden-

tified two characteristic motifs, the "white flower" (WF) (Refs. 22 and 23) and the pentagonal "dark stars" (DSs).[24,25] The WF motif has been shown to be formed by truncated pseudo-Mackay clusters which are, together with Bergman clusters (BCs), the constituting elements of the bulk icosahedral structure. This assignment is confirmed by detailed simulations of the STM contrast based on *ab initio density-functional* calculations.[21] These simulations also show that the DS corresponds to a surface vacancy originating from the irregular atomic arrangement around the low-coordinated Mn atoms in the center of the pseudo-Mackay clusters.

The quasiperiodic structure of the surface can be described by a planar tiling. The choice of this tiling is, however, not unique. One possible choice relating to the cluster structure of the bulk quasicrystal is the Penrose P1 tiling[26] consisting of regular pentagons, pentagonal stars, boats, and thin golden rhombi. The vertices of the P1 tiling coincide with the centers of the Bergman clusters projected to the surface plane, and the centers of the pentagonal tiles correspond to the positions of the pseudo-Mackay clusters. Another choice of the quasiperiodic tiling is a decagonal DHBS (decagon-hexagon-boat-star) tiling sharing vertices with the P1 tiling. For alkali-metal monolayers it has been shown that an initial structure defined as a decorated P1 tiling transforms during relaxation to a DHBS tiling.

In Sec. II we briefly summarize results of our previous STM investigations of initial adsorption of Pb on the fivefold Al-Pd-Mn quasicrystal surface. In Sec. III the computational setup and the construction of structural models of Pb layers at two different coverages are described. The quasiperiodic ordering and the structural properties of the monolayers are discussed. Sections IV and V are devoted to the investigation of energetics and the electronic properties of the monolayers, respectively.

II. EXPERIMENTAL STM STUDIES

In previous experimental studies[14,16] the growth of a Pb monolayer on the fivefold surface of the Al-Pd-Mn quasicrystal has been investigated in detail. We have observed that at the early stages of the deposition, Pb adatoms diffuse across terraces and form nanosized islands. Because of their protruding "arms" and their overall pentagonal shape, these clusters were dubbed SF. These clusters exhibit a similar size and orientation across successive terraces, independently of the deposition rate. These observations suggest heterogeneous nucleation at preferred nucleation sites. The local atomic arrangements around single Pb atoms (i.e., at the first stage of the SF nucleation) and around completed SF motifs have been investigated on several atomically resolved STM images. It appears that these pentagonal islands are located on equatorially truncated pseudo-Mackay clusters surrounded by five truncated Bergman clusters, i.e., on top of WF motifs. This conclusion is supported by additional measurements of the SF-to-SF distances across terraces.[16]

At later stages of the deposition in the submonolayer coverage regime, the largest distinguishable pentagonal features can be understood as a set of SF clusters. Similarly, the skeleton of a completed Pb monolayer can be seen as a self-assembled network of the SF clusters. As the size of the SF cluster can be characterized by a pentagon with the edge of the P1 tiling (7.76 Å), it is legitimate to assume that the atomic structure of the monolayer can be described as a decorated P1 tiling. In STM images of the full monolayer one can observe striking bright spots. In Fourier-filtered images[14] the distribution of these bright spots can be characterized by a τP1 tiling, which is the P1 tiling with an edge length inflated by a factor $\tau=1.6018$ (the golden mean). The quasiperiodic structure of the Pb monolayer can be thus characterized on a larger scale by the τP1 tiling. An interesting structural feature observed in the complete Pb monolayer is a WF motif, similar to that observed in STM images of clean fivefold surface, but again scaled by a factor τ. We denote this motif as τWF and in Sec. III the details of its structure will be resolved. The inspection of the STM images also reveals a rather large degree of structural disorder in the monolayer (see Fig. 1). Although part of the disorder could have a thermal origin, a significant contribution probably comes from an imperfect match between the local structures of the substrate and the adlayer.

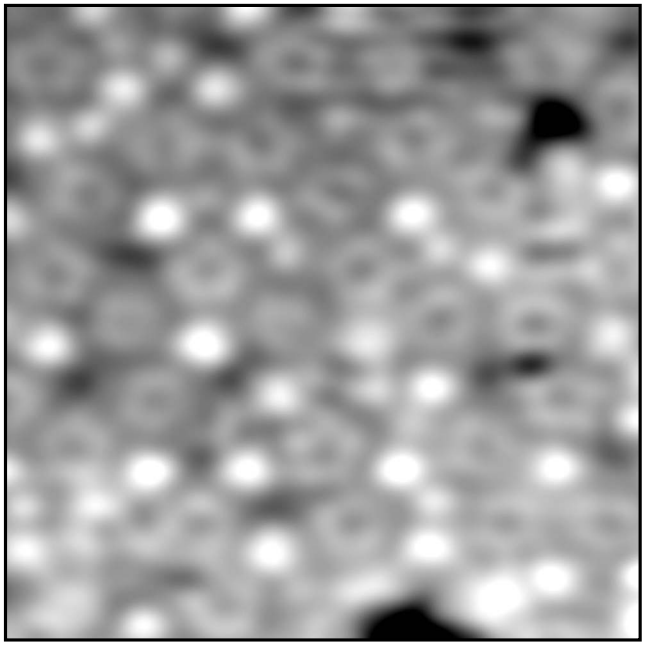

FIG. 1. 10 nm$\times$10 nm STM image of a Pb monolayer deposited on the fivefold surface of the *i*-Al-Pd-Mn quasicrystal at 653 K.

III. MODELING THE STRUCTURE OF THE Pb MONOLAYER

A. Computational setup

The theoretical modeling of the structure of the Pb monolayer is based on density-functional theory. We have used the Vienna *ab initio* simulation package VASP (Refs. 27 and 28) to perform *ab initio* electronic-structure calculations, structural optimizations, and simulation of the STM images. More details of the method can be found in our previous papers.[16,18,19]

B. Structure of the clean fivefold surface of Al-Pd-Mn

A model for the surface has been derived from the KGB model[29,30] of bulk *i*-Al-Pd-Mn. The atomic structure of the fivefold surface is derived from the structure of an icosahedral approximant by cleaving along a plane perpendicular to one of the fivefold axes, at a point where the distances between neighboring planes is the largest. Details of construction of models of the bulk and the surface can be found in our previous papers.[19,21,30]

Figure 2(a) shows the atomic structure of the top atomic plane of the fivefold Al-Pd-Mn surface, as derived from the 5/3 approximant to the bulk quasicrystal. The quasiperiodic arrangement of atoms in the top plane can be described either by a P1 tiling consisting of pentagons, pentagonal stars, boats, and thin rhombi or by a planar DHBS tiling composed of D, squashed H, B-shaped tiles, and pentagonal S.[19] The top plane is Al rich and contains a few Mn but no Pd atoms. This chemical composition has also been confirmed experimentally.[31] The centers of the D tiles can be occupied either by Mn or by Al atoms, and their vertices correspond to the positions of Pd atoms in subsurface layers. The decagonal tiles have a direct relation to the WF features seen in the STM images of the clean surface. In the topmost plane the vertices of the D tiles coincide with the centers of small pentagons of Al atoms (with an edge length of 2.96 Å) forming the "leaves" of the white flowers. The centers of WFs represented by the D tiles are the nucleation centers for the Pb starfish clusters. The pentagonal-S tiles in Fig. 2(a) have two orientations. They are decorated by five Al atoms located in arms of the star plus 0–2 other Al atoms in the interior of the tile. The irregular decoration of the S tiles is a consequence of the low and irregular coordination of Mn atoms in the centers of the pseudo-Mackay clusters, located below or above the surface. The S tiles with empty interiors are seen in STM images of the clean surface as DSs.

Alternatively, the structure of the surface can be described by a τ-scaled τP1 tiling Fig. 2(a) shows the P1 and the τP1 tiling and their relation to the DHBS. The centers of the D tiles coincide with the vertices of the τP1 tiling. The τP1 tiling with an edge length of 12.55 Å describes the quasiperiodic ordering of the Pb monolayer.

Our previous adsorption studies have been performed on a slab model of the fivefold surface derived from the 2/1 or 3/2 approximants to the quasicrystalline Al-Pd-Mn structure.[18–20] The 2/1 approximant is too small for modeling a quasiperiodic ordering at the scale of the τP1 tiling. The size of the 3/2 approximant would be sufficient but the structure of the surface derived from the 3/2 approximant that we used in our previous studies[19,32] cannot be interpreted as a part of the τP1 tiling. We have used the same approach in our present studies but to get a model of the surface with τP1 ordering we had to prepare a special 3/2 approximant derived from the larger 5/3 approximant. The two surface models provide us with a larger variety of the atomic configurations that occur on the infinite quasicrystalline surface. From the 5/3 model of the surface we cut a rectangular area with the size of the 3/2 approximant (32.86 Å $\times$ 38.63 Å) and enforced periodic boundary conditions, see Fig. 2(b). (As the occupation domains of the 5/3 and 3/2 approximants differ only a

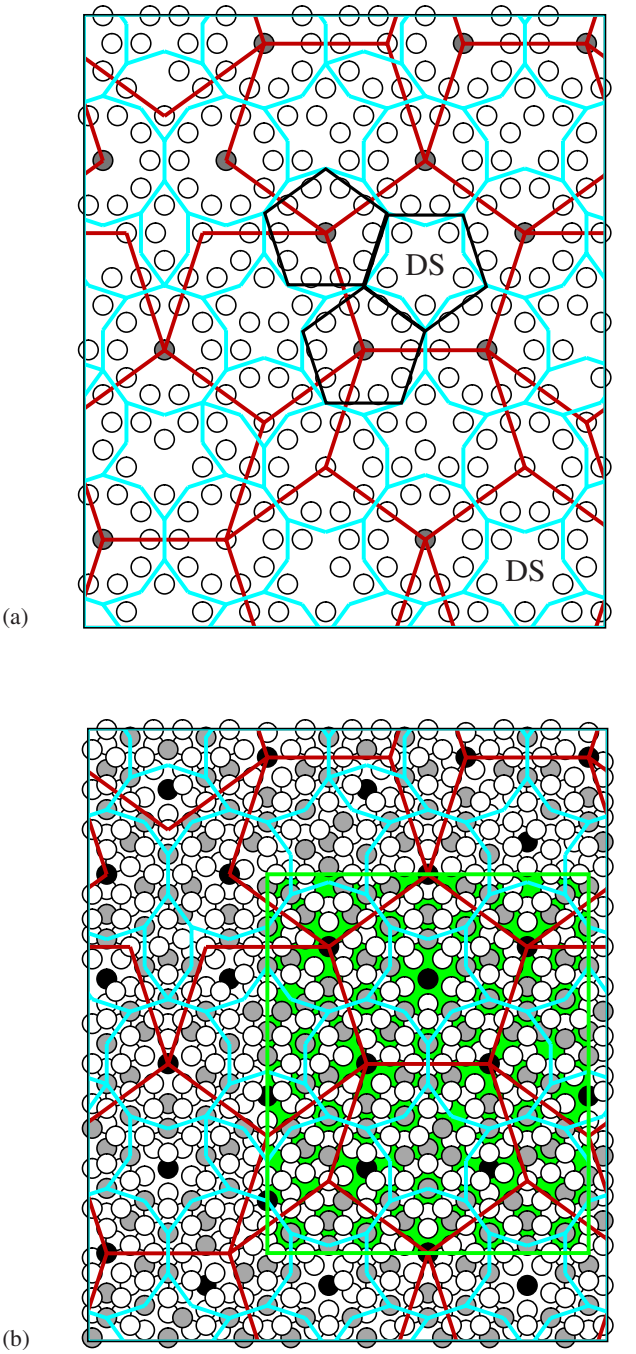

FIG. 2. (Color online) (a) The atomic structure of the top atomic plane of the fivefold Al-Pd-Mn surface. The quasiperiodic arrangement of atoms in this plane can be described either by a decagonal DHBS tiling (cyan) or by a P1 tiling (black, only a part is shown). The centers of the decagonal tiles of the DHBS tiling or of the pentagonal up tiles of the P1 tiling are occupied either by Mn (closed circles) or Al (open circles) atoms, and they coincide with the vertices of the τP1 tiling (red). DS marks configurations of atoms that in STM images are seen as the dark stars. (b) The fivefold Al-Pd-Mn surface with the inclusion of subsurface planes of atoms: Al—open circles, Pd—gray circles, and Mn—closed circles. The model of the surface has been constructed from the 5/3 approximant to the bulk quasicrystal. For adsorption studies we used a smaller 3/2 approximant (the green marked rectangular area) cut from the 5/3 approximant.

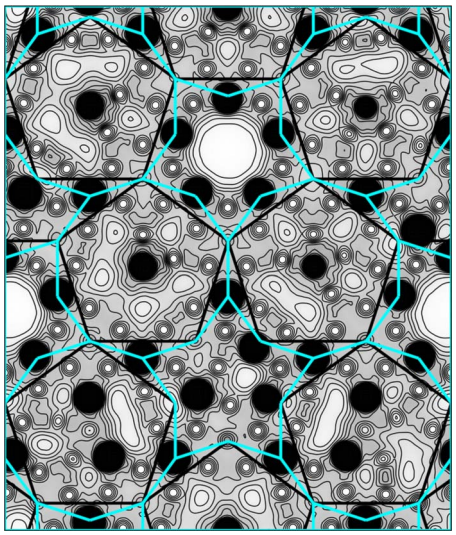

FIG. 3. (Color online) The charge-density distribution at the fivefold surface of Al-Pd-Mn (model L). Transition metal atoms are seen as dark spots, Pd as larger and Mn as smaller spots. The quasiperiodic ordering can be represented by the DHBS (cyan) or the P1 (black) tiling.

little in perpendicular space, the enforced boundary conditions lead only to a few interatomic conflicts that were resolved "manually," i.e., the position of the conflicting atom was flipped to a near symmetry equivalent site). The position of the rectangular area can be arbitrarily chosen. We have selected a part of the surface that contains τP1 pentagons of both orientations. To distinguish this model of the surface from the previous model we shall denote this new model as L. The model used in previous work[32] will be referred as model H. With model L we shall investigate formation of a Pb layer at a lower coverage. Model H is used as a substrate for a layer at a higher coverage. Both models of the surface have a form of a slab. The thickness of the slab is 4.2 Å and it consists of five atomic planes. This thickness is sufficient for the simulation of STM images (i.e., for reproducing the charge-density distribution several angstroms above the surface). The positions of all atoms in the slab, except for the atoms in two bottom planes, were relaxed together with the positions of the adsorbed atoms. Neighboring images of the slab are separated by a 14 Å thick vacuum layer. The computational cell has an orthorhombic shape, and it contains 350 substrate atoms plus up to 106 adsorbed Pb atoms.

C. Structure of Pb adlayers

For determining the location of possible adsorption sites it is helpful to look first at the valence charge-density distribution at the clean surface. Figure 3 shows the charge-density distribution at the surface calculated for our model L. We note that the other model H has been described in detail in our previous papers.[19–21,32] The most peculiar features of the surface charge-density distribution are large charge-density minima inside some S tiles. These charge depletions correspond to surface vacancies seen in the STM images as DSs. Inside the D tiles one can observe also smaller charge-density minima arranged around the center with approximate pentagonal symmetry. These hollow sites have been found as preferable adsorption sites for alkali metals atoms[19] but Pb atoms in the SF cluster prefer bridge positions between these sites forming thus a pentagon with the opposite orientation. These sites can also be considered as threefold hollows between two Al atoms in the surface layer and a third Al atom located slightly below the surface.[16] Significant adsorption sites are also the vertices of the D tiles. Half of these vertices are occupied by Pd atoms located 0.48 Å below the top layer, and the remaining vertices are hollow sites surrounded by five Al atoms and located above a Pd atom located deep (1.26 Å) below the surface plane. They coincide with centers of the BCs and form vertices of the pentagons of the P1 tiling.

Figure 4(a) shows a view on the surface of the model L with one adsorbed SF cluster. Figure 4(b) is the corresponding STM image calculated for a constant current and a scanning voltage of +2 V. The atomic structure of the SF cluster has been determined by looking for the configurations with the highest adsorption energy per Pb atom and by comparison of the experimental and calculated STM images (details can be found in our previous study[16]). The geometry of one SF cluster corresponds to a pentagon of the P1 tiling. The P1 tiling consists of two types of pentagons differing in orientation. We distinguish them as pentagons pointing "up" and "down." We shall denote them as uP and dP tiles, respectively. The centers of both types of pentagons correspond to a Mn [alternatively also Al, see Fig. 2(a)] atom in the center of a pseudo-Mackay cluster. For the uP the Mn(Al) atom is located in the surface layer and for the dP it is located 2.56 Å below the surface. The orientation of the SF cluster corresponds to the uP pentagon.

While the decoration of the uP pentagons is known from the resolved atomic structure of the experimentally observed SF clusters the decoration of dP pentagons by Pd adatoms is not obvious. As the surface of the dP pentagon is formed by atoms from the irregular low coordinated first shell of the pseudo-Mackay cluster the atomic structure of the substrate inside dP is not regular. Some of the dP pentagons are centered by a surface vacancy arising from the low coordination of the Mn atoms just below. (These are just those pentagons that correspond to DSs seen in STM images of the substrate.) Above a central Pb atom filling the vacancy the dP tiles can accommodate five Pb atoms forming a regular pentagon. This pentagon can adopt one of two possible orientations discussed below. The decoration of all other tiles is to a large extent enforced by the decoration of the pentagonal tiles. We have considered many possible configurations of adsorbed Pb atoms. The stability of the adsorbed Pb layer was probed by performing a conjugate-gradient relaxation of the structure of the adlayer/substrate complex under the action of the Hellmann-Feynman forces. Because of the limited space we present results for two models only, one for a lower coverage of 0.066 atoms/Å^2 ($\Theta \approx 0.5$, the atomic density of the Al-Pd-Mn surface layer is 0.136 atoms/Å^2) and one for a densely packed structure with a 0.083 atoms/Å^2($\Theta \approx 0.63$). We note that the experimentally measured coverage of 1 ML at full saturation is $\approx$0.09 atoms/Å^2.

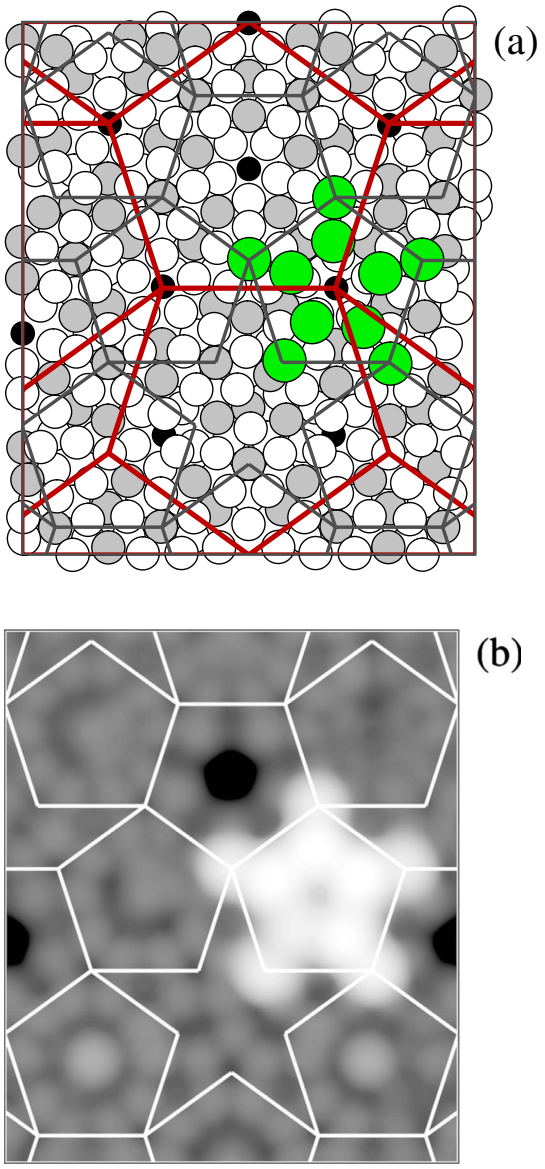

FIG. 4. (Color online) (a) A view on the fivefold Al-Pd-Mn surface (model L) with an adsorbed SF cluster consisting of ten Pb atoms. (b) A simulated STM image of the SF cluster calculated for a constant current and scanning voltage of +2 V.

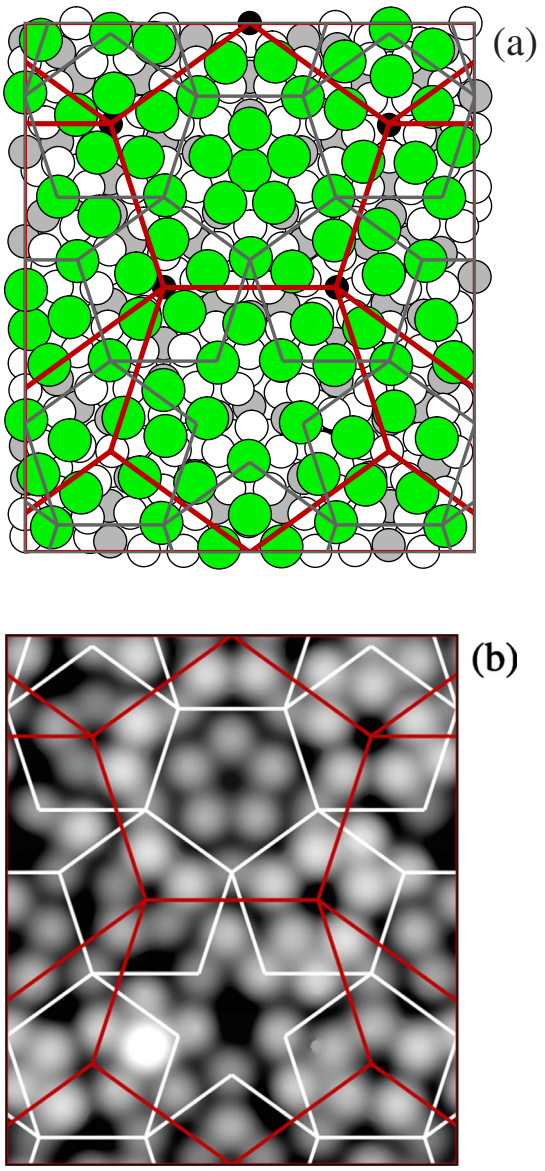

FIG. 5. (Color online) (a) The structure of adsorbed Pb monolayer at the coverage of 0.066 atoms/Å^2 (model L). The quasiperiodic ordering is represented by the P1 (black lines) and τP1 tiling (red lines). (b) A simulated STM image of the Pb monolayer in (a).

1. Intermediate coverage—$\Theta \approx 0.5$

Figure 5(a) shows a relaxed configuration of atoms at the lower coverage. In the initial structure SF clusters have been placed on all up pentagons of the P1 tiling. For the positions of the remaining Pb atoms we followed our earlier work on Bi and Sb monolayers on this surface[20] where the vertices and mid-edge positions of the P1 tiling have been identified as the energetically most favorable adsorption sites (adatoms also bind very strongly to Mn atoms in the surface layer but they occur only in the centers of the up pentagons which are already occupied by the SF clusters). The positions on the edges forming the angles of the S and B tiles cannot be occupied simultaneously because of an unphysically short distance. In these cases the initial positions are bridge positions between these mid-edge sites (corresponding to a vertex position of the DHBS tiling). Pb atoms were also placed into all surface vacancies—in the present model such vacancies exist in the center of the down pentagons (see also Fig. 3). This decoration leads to a coverage of $\Theta \approx 0.5$ (density 0.066 atoms/Å^2).

Relaxation largely preserves the structure of the SF clusters and the position of the adatom placed at the P1 vertices but the atoms initially placed at mid-edge positions move toward the interior of the dPs, forming a pentagon in up orientation. A Pb atom filling a surface vacancy is located just below the center of the pentagon. Obviously the formation of these pentagonal motifs is a consequence of significant attractive lateral interactions between the Pb atoms. In principle, the dPs could also be decorated by Pb pentagons in a down orientation. We have tested both orientations and found that the up orientation at this coverage provides a bet-

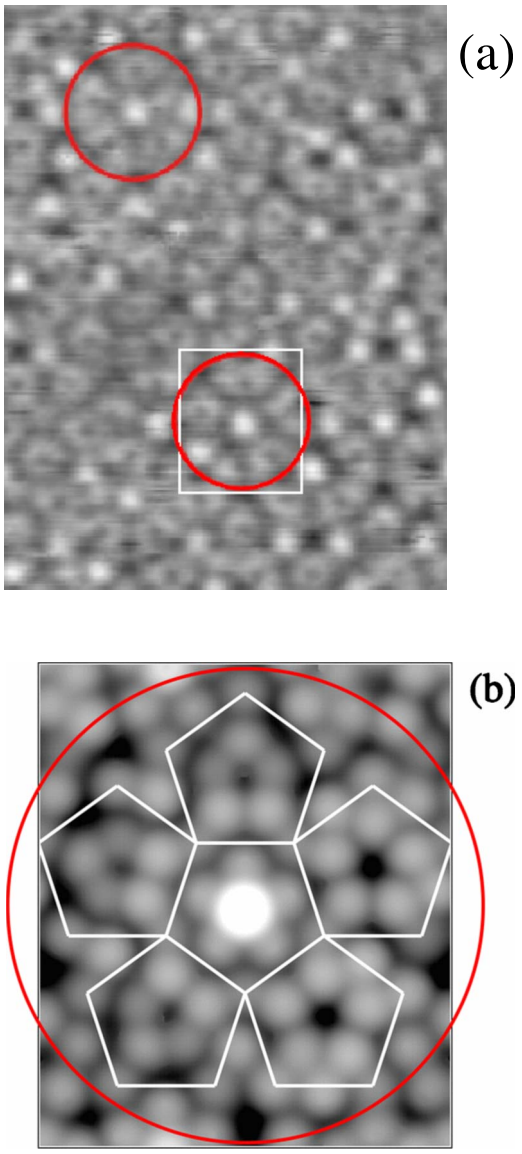

FIG. 6. (Color online) (a) A 12.0 nm × 15.7 nm high-resolution STM image of the adsorbed Pb monolayer. Two τ-scaled WF motifs are marked by red circles. (b) A simulated STM image of the τWF motif. The skeleton of the τWF motif consists of five uP tiles of the P1 tiling arranged around one dP tile. The size of the white rectangle in part (a) corresponds to the size of the structural model (b).

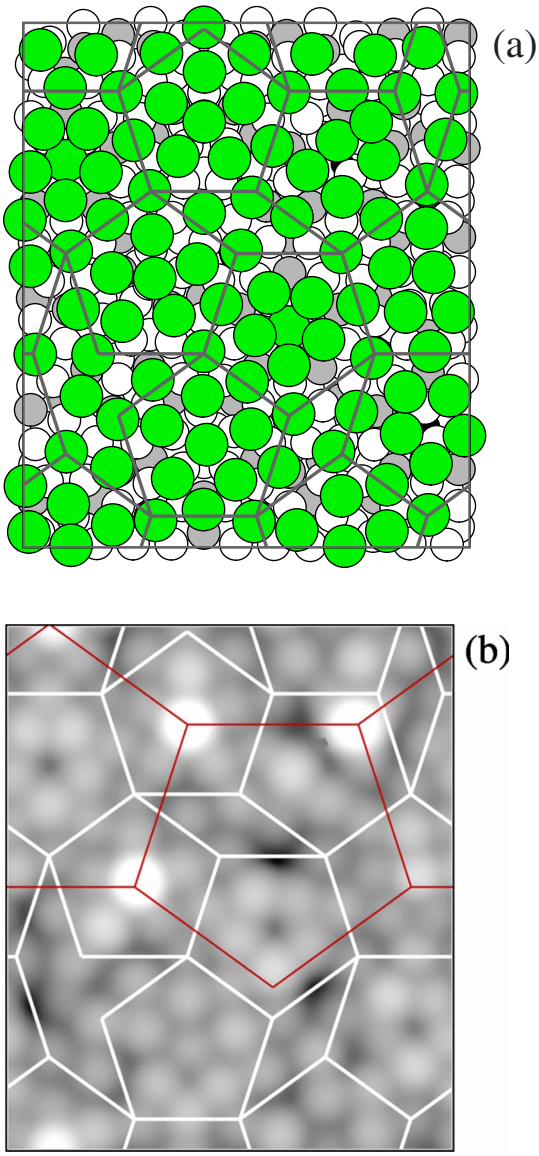

FIG. 7. (Color online) (a) The structure of adsorbed Pb monolayer at the coverage of 0.083 atoms/Å^2 (model H). The quasiperiodic ordering is represented by the P1 (black lines). (b) A simulated STM image of the Pb monolayer from the previous figure. The bright spots can form vertices of the τP1 tiling.

ter agreement with the experimental STM images.

The upper part of Fig. 5(a) shows a dP pentagon surrounded by five uP pentagons. Such a configuration corresponds to the experimentally observed τ-scaled WF, see Fig. 6(a). The Pb atom in the center of the dP fills a surface vacancy [see Fig. 5(a)], it is located below the five Pb atoms forming the pentagon. Obviously one additional Pb atom can be adsorbed in the hollow site formed by the Pb pentagon in the center of the dP. This atom is located slightly above its five neighbors and generates the bright spot seen in many of the τ-scaled WFs [Fig. 6(b)].

2. Saturation coverage—$\Theta \approx 0.63$

The highest experimentally observed density of a Pb monolayer is 0.09 atoms/Å^2. To achieve this high density, additional Pb atoms have to be accommodated. We have constructed a model for a high-density overlayer based on the surface model H. A higher coverage was achieved by the following steps: (i) Pb atoms are placed into the center of the SF clusters occupying the uP tiles. (ii) If the Pb pentagons decorating the interior of the dP tiles are oriented in the down direction, additional Pb atoms may be placed into the centers of the edges shared by a uP and a dP pentagon. This leads to a density of 0.083 atoms/Å^2, close to the experimental saturation.

The relaxed model of a Pb monolayer with this high density and its simulated STM image are presented in Fig. 7(a). In the STM image bright spots appear in the centers of some uP pentagons. The explanation of the origin of these bright spots can be found in the structure of the substrate. On the

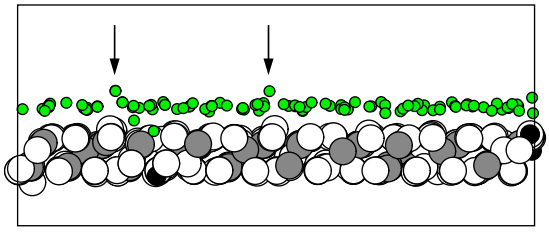

FIG. 8. (Color online) A side view on the Al-Pd-Mn substrate with the adsorbed Pb monolayer. Al—open circles, Pd—gray circles, and Mn—closed circles. Position of Pb atoms is indicated by small green circles. The protruding Pb atoms marked by arrows are seen as bright spots in STM images. Figure demonstrates also the corrugation of the Pb monolayer.

clean surface the centers of the D tiles [Fig. 2(a)] or, equivalently, of the uP tiles (Fig. 3) are occupied either by Mn or Al. The bright spots in the STM images of the Pb monolayer appear in the uP tiles centered by Al atoms. The uP tiles centered in the substrate by Mn sites give only weak contrast. The central Al atom is less strongly bonded to the neighboring Al atoms in the substrate than the Mn atom. After the structural relaxation of the adlayer/substrate complex the central Mn atoms remain approximately in the surface plane while the central Al atoms are lifted by ≈ 0.6 Å above the surface plane. Consequently the Pb placed on top of these Al atoms move above their neighbors, see Fig. 8. The distance between two neighboring bright spots corresponds to the edge of the τP1 tiling. The bright spots can thus form the vertices of a τP1 tiling as experimentally observed, see Fig. 3 in Ref. 14.

The bright spots seen in the STM images can also originate from protruding Pb atoms. The regular decoration in some tiles can be substantially distorted. In Fig. 7(a) the regular pentagonal decoration of the dP tile at the upper right corner of the figure was rearranged and one Pb atom was pushed up. A similar protruding Pb atom can be found also in model L, see Fig. 5(b). A bright spot originating from an irregular arrangement of atoms in the monolayer can appear at any position. However, the observed defect in the arrangement of atoms can also be interpreted in a different way. A decoration defect in one tiling model can be a regular site in another tiling. The formation of the defect observed in Fig. 7(b) can be interpreted as a reordering of the quasiperiodic arrangement in the P1 tiling to another quasiperiodic arrangement at a larger scale described by the τP1 tiling. A similar reordering we observed also in quasiperiodic alkali-metal monolayers[19] on the same Al-Pd-Mn surface where the quasiperiodic P1-type ordering spontaneously transformed to DHBS ordering upon relaxation.

A good measure of the regularity of a monolayer is its corrugation. The corrugation of an adlayer can be characterized by the mean-square deviation σ of the positions of the atoms from their average height h. The corrugation is imprinted partly by the corrugation of the substrate and partly by the different strength of the adsorbate/substrate bonds at different sites. The corrugation of the clean fivefold Al-Pd-Mn surface itself was estimated[18] to be ≈ 0.22 Å. Figure 8 shows a side view of the Pb monolayer, visualizing its corrugation. Besides the protruding Pb atoms responsible for the bright spots in the STM images the largest deviations from an in-plane position are Pb atoms trapped in charge-density minima, particularly in the surface vacancies. If one excludes from the monolayer the Pb atoms inside these surface vacancies, the mean-square deviation of the positions of the Pb atoms from their average height above the surface is $\sigma = 0.301$ Å. This value can be compared with the value of 0.122 Å characterizing the corrugation of the Na monolayer on the fivefold Al-Pd-Mn surface.[18] While the corrugation of the Na monolayer was found to be smaller than the corrugation of the clean substrate the corrugation of the Pb monolayer is larger. The Pb monolayer is thus less regular than the Na monolayer. Although the size of Pb atoms ($d_{\mathrm{Pb}} \approx 3.39$ Å, estimated from the nearest-neighbor distance in the low-temperature crystalline phase) is smaller than the size of Na ($d_{\mathrm{Na}} \approx 3.77$ Å) the average height of Pb atoms in the monolayer above the surface plane $h = 2.32$ Å is larger than the height $h = 2.19$ Å of the Na monolayer. This can be explained by the fact that in the adsorbed Na monolayer all atoms occupy hollow sites on the *i*-Al-Pd-Mn surface, whereas in the Pb monolayer the only Pb-occupied hollow sites are the vertices of the P1 tiling and most other Pb adatoms decorating interiors of the tiles occupy bridge positions.

IV. ENERGETICS OF THE ADSORBED Pb MONOLAYER

In our previous work[16] it was found that during the initial stages of Pb deposition SF clusters consisting of ten atoms are formed. Calculations of binding energies have confirmed that the SF cluster is a stable structure with an average binding energy of −4.06 eV per Pb atom in the cluster. This value can be compared with the average binding energy of a Pb atom in the saturated monolayer. For the monolayer grown on the substrate model H shown in Fig. 7(a) the average binding energy is −3.97 eV per Pb atom. As the skeleton of the monolayer consists of a network of SF clusters, the similar values of the binding energies is not surprising. A contribution to the average binding energy of a Pb atom in the monolayer comes from atoms filling surface vacancies. The binding energy of an isolated Pb atom adsorbed in a surface vacancy is −4.64 eV, i.e., it is substantially higher than the average binding energy. However, the fraction of Pb atoms occupying surface vacancies is quite small, between 1% and 2% in our models. As the surface vacancies act as trap sites strongly binding the adatoms, it could be expected that these sites are occupied in the very early stages of deposition. However, a close inspection of STM images shows that this appears not to be the case. DS motifs corresponding to the surface vacancies can be well recognized in the vicinity of the adsorbed SF clusters. On the other hand, the simulated STM images show that a single Pb atom occupying a surface vacancy does not give any special contrast. The attractive site in the surface vacancy is atop the Mn atom deep (2.56 Å) below the surface plane and therefore at the deposition temperature (formation of the SF clusters was observed in wide range of temperatures from 57 up to 650 K) this site can be inaccessible to atoms diffusing across the

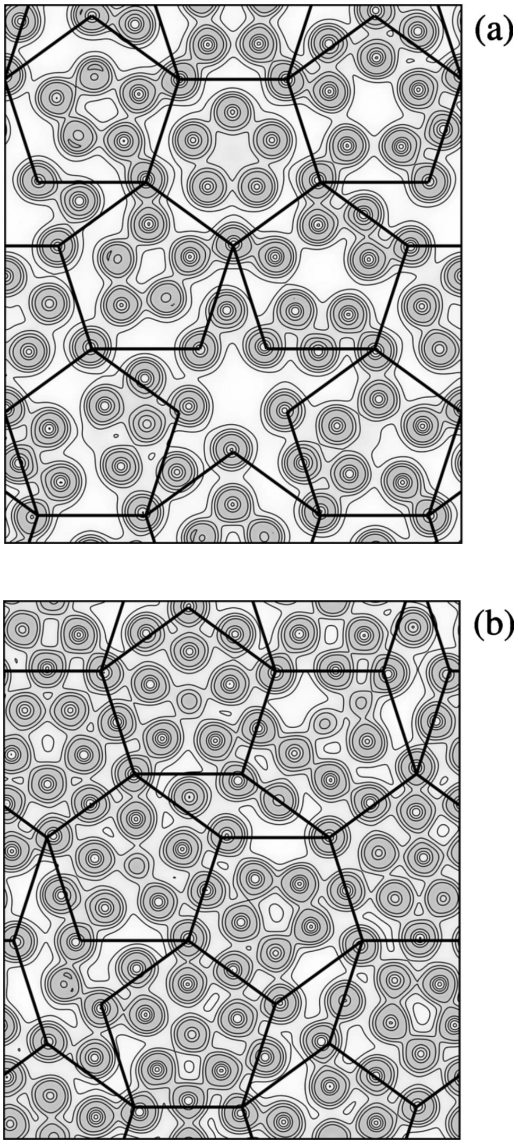

FIG. 9. The electron-density distribution of Pb monolayers for both models: (a) model L (coverage of 0.066 atoms/Å^2) and (b) model H (coverage of 0.083 atoms/Å^2). The quasiperiodic ordering is represented by the P1 tiling.

surface for kinetic reasons. Part of the surface vacancies may be filled by adatoms, simultaneously with the formation of the SF clusters, but the majority of them will be occupied only during later stages of the deposition.

V. ELECTRONIC PROPERTIES OF QUASIPERIODIC Pb MONOLAYERS

Figure 9 shows the electron-density distribution of Pb monolayers for both models—model L representing a monolayer with a density of 0.066 atoms/Å^2 and model H with a density of 0.083 atoms/Å^2. Charge-density maxima represent Pb atoms, charge-density overlaps arise from the formation of covalent bonds between adatoms. At the lower coverage, most Pb atoms bind to two or three Pb neighbors, leading to a network of interlinked -Pb-Pb- chains and clusters. At the higher density the Pb-Pb coordination increases and a denser network of lateral bonds in seen.

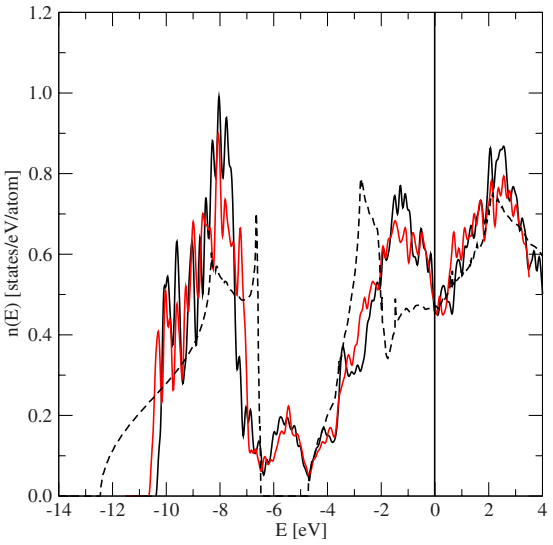

FIG. 10. (Color online) The DOS of Pb monolayer for coverage of 0.066 (black line) and 0.083 atoms/Å^2 (red line). The dotted line is the DOS of fcc Pb.

Pb atoms have two 6*s* and two 6*p* valence electrons. Because of relativistic effects, the difference in the eigenvalues between the 6*s* and 6*p* states is larger than for the lighter group-IV elements and therefore the formation of sp^3 hybrids is energetically unfavorable. These relativistic effects also contribute to stabilize the face-centered-cubic (fcc) structure over the diamond structure adopted by the lighter elements,[33] and they are also important for understanding the electronic structure of the quasiperiodic Pb monolayers. Figure 10 presents the partial density of states (DOS) of Pb atoms in the adsorbed monolayers calculated for both coverages considered, compared with the DOS of fcc Pb. A peculiar feature of the DOS of crystalline Pb is that the *s* and *p* bands are separated. The *s* band extends from −12.45 to −6.5 eV. As the bottom of the *p* band is at −4.42 eV a gap of 1.78 eV between the *s* and *p* bands is formed. The internal gap separating the *s* and *p* bands is not structure induced, it is found even in the electronic DOS of liquid Pb.[34] The structure of the DOS of fcc Pb is strongly modulated by the van Hove singularities. The Fermi level falls in a region between two van Hove peaks at −2.72 and 2.16 eV.

The gross features in the DOS of the quasiperiodic monolayers are reminiscent of those of fcc Pb. The *s* band of the monolayers of both coverages shows a DOS maximum at ≈−8 eV. Its width is narrower compared to crystalline Pb, reflecting the lower Pb-Pb coordination. The internal *s*-*p* band gap is filled because of the hybridization of the Pb orbitals with substrate states.

The most interesting region of the DOS is around the Fermi level. Here the DOS of both monolayers exhibits a clear pseudogap. It is tempting to assign the pseudogap to the quasiperiodic ordering of the atoms in the monolayer. In previous work[16] the electronic structure of the Pb monolayer has been probed using scanning tunneling spectroscopy (STS) and ultraviolet photoelectron spectroscopy (UPS).[14] A

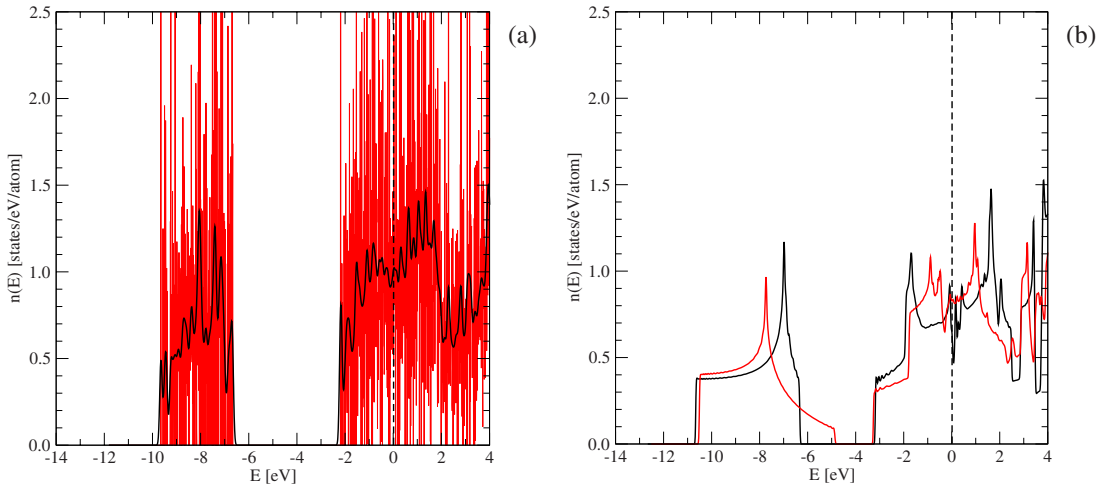

FIG. 11. (Color online) Comparison of the DOS of unsupported quasiperiodic (a) and periodic (b) Pb monolayers. The unsupported quasiperiodic Pb monolayer was obtained from the model H by removing the substrate atoms. In part (a) the spiky DOS of the quasiperiodic monolayer (red) was smoothed by a Gaussian broadening with the parameter $\sigma=0.05$ eV (black line). In part (b) the DOS of triangular (black) and square (red) lattices are presented. The lattice parameters of both periodic lattices are equal to their equilibrium values.

pseudogap (DOS minimum) at the Fermi level has been observed and it was suggested that it originates from the quasiperiodic structure of the monolayer. The calculated electronic structure of the monolayers confirms the existence of the pseudogap at the Fermi level. The existence of a deep pseudogap in the quasiperiodic layer can be contrasted with the electronic structure of liquid Pb where the DOS was found to be essentially constant in a wide range of ± 4 eV around the Fermi level.

A pseudogap at the Fermi level has been observed in the electronic structure of many quasicrystals[35–39] and therefore it has often been assumed that it might be a generic property of quasicrystals. It was suggested that the formation of the pseudogap is driven by a Hume-Rothery mechanism. However, it is also known that a similar pseudogap exists also in many crystalline structures[40,41] so that it is obvious that the pseudogap is not a property specific to quasicrystals.

To shed light on the origin of the pseudogap in the DOS of the Pb monolayer supported on the surface of *i*-Al-Pd-Mn and to assess its importance for its stability, we have calculated the DOS of a free-standing quasiperiodic monolayer, a periodic triangular monolayer, and a square Pb monolayer. The structure of the quasiperiodic Pb layer has been taken from model H (see Fig. 7) by removing the substrate and keeping the positions of the Pb atoms fixed. The unit cell of this model measures 38.63 Å $\times$ 32.86 Å and contains 106 Pb atoms (density 0.083 atoms/Å^2). The periodically repeated layers are separated by a distance of 16.5 Å. The DOS was calculated using a $4\times4\times1$ **k**-point mesh. Figure 11(a) demonstrates that the DOS of the freestanding quasiperiodic Pb monolayer has a very spiky character. The eigenstates have almost no dispersion. The spikiness of the DOS of quasiperiodic structures is well known and has been discussed in literature for many years.[35,37,38,42–44] In real quasicrystals the spikiness is to a large extent smoothed out[44] as confirmed also by photoemission studies.[43] On the other hand the spiky aspect of the DOS has been recently confirmed on the nanometer scale using scanning tunneling spectroscopy on the fivefold surface of the *i*-Al-Pd-Mn quasicrystal.[45] Figure 11(a) also shows that after a Gaussian broadening with $\sigma=0.05$ eV the DOS of the quasiperiodic Pb layer shows only a shallow minimum at the Fermi level. Hence the deeper pseudogap of the supported Pb layer shown in Fig. 10 is imposed by the binding to the quasiperiodic substrate.

For the periodic Pb monolayers the in-plane lattice constants have been relaxed. For the triangular layer we calculate an equilibrium lattice constant of $d=3.30$ Å, corresponding to a density of 0.106 atoms/Å^2. For the square monolayer we find $d=3.12$ Å and a density of 0.103 atoms/Å^2. The binding energies are -3.11 eV/atom for the triangular and -2.99 eV/atom for the square monolayer, to be compared with an average binding energy of -2.78 eV/atom for the free-standing quasiperiodic Pb layer. Hence both periodic monolayers have a lower energy and higher density than the quasiperiodic layer. The electronic DOS was calculated based on Brillouin-zone integrations using a very fine **k**-point mesh ($45\times45\times1$), as the size of the Brillouin zone of the periodic models is much bigger then that of the quasiperiodic approximant, and correspondingly larger **k**-point sampling is necessary. The calculated DOS is shown in Fig. 11(b) and is characterized by very sharp DOS minima close to the Fermi edge. Hence the periodic Pb monolayer shows a pseudogap at the Fermi level while the quasiperiodic layer does not.

From the comparison of the DOS of supported (Fig. 10) and unsupported [Fig. 11(a)] Pb monolayers it is obvious that the states in the gap between 6*s* and 6*p* states in the supported monolayer, as well as the pseudogap at the Fermi level originate from the hybridization of the Pb states with Al states from the substrate. This is also supported by the results of UPS (Ref. 14) which demonstrated that the intensity profiles at the Fermi level are identical for clean and Pb-covered Al-Pd-Mn surfaces—the UPS intensity contains contributions both from the Pb layer and from the substrate. STS on the other hand probes only the Pb overlayer and suggests that the width of the pseudogap is larger in the Pb overlayer than on the clean substrate. This observation might be attributed

to relativistic effects which have not been included in our calculations. For the heavy elements the relativistic spin-orbit coupling causes a splitting of the $6p$ band into $p^{1/2}$ and a $p^{3/2}$ components separated by a deep minimum in the electronic DOS. For tetravalent Pb the minimum is located precisely at the Fermi level. The importance of spin-orbit coupling in the interpretation of the electronic spectra of the heavy elements has also been confirmed for molten Pb and Bi where the UPS data show a clear DOS minimum at a band filling corresponding to two $6p$ electrons, whereas the DOS calculated without spin-orbit coupling is essentially constant throughout this energy range.[34,46]

VI. MULTILAYER GROWTH

A striking experimental observation[14] is that once a full monolayer has been completed, no further Pb atoms are adsorbed. This is in contrast to the multilayer growth observed for alkali[15] or Bi (Ref. 13) films on the fivefold *i*-Al-Pd-Mn surface. During the deposition process the rate of Pb adsorption decreases with increasing coverage and vanishes once saturation of one monolayer has been achieved. No further growth was observed over a wide range of deposition rates and substrate temperatures. This "nonsticking" property of the Pb monolayer demands an explanation.

The growth of an adlayer depends on two essential factors: (i) a strong binding of the adatoms to the substrate and (ii) the ability to dissipate the kinetic energy through atomic collisions leading to the excitation of phonons in the substrate. Both conditions are met for the growth of a first Pb monolayer on the clean surface of the quasicrystal. The adsorption energy of Pb atoms is about 4 eV/atom—this is a substantial fraction of the binding energy in fcc Pb of 7.32 eV/atom. The phonon density of states of *i*-Al-Pd-Mn measured by incoherent inelastic neutron scattering[47] extends up to energies of about 60 meV. The strong interaction of the adatoms with the substrate leads to an efficient dissipation of their kinetic energy via the excitation of high-energy phonons.

The condition for the growth of a second Pb layer is rather different. We have calculated the adsorption energies of Pb atoms deposited on top of a saturated monolayer. For five isolated Pb adatoms adsorbed at random positions on the first monolayer on the substrate H [Fig. 7(a)] we found an average binding energy of 2.68 eV per Pb atom. This is only slightly more than one third of the binding energy in crystalline Pb. The highest phonon energies in fcc Pb are only about 9 meV (Ref. 48) and since the binding in the Pb monolayer is weaker than in the bulk metal, it appears to legitimate to assume that this is also an upper limit to the energy of phonons in the quasiperiodic monolayer. Dissipation of the kinetic energy of atoms impinging on a completed monolayer will therefore be much less efficient because it requires the multiple excitation of low-energy phonons.

As seen in Fig. 7(a) a saturated Pb monolayer at a coverage 0.083 atoms/Å^2 is very compact, and the surface corrugation is rather low. Barriers for the diffusion of adatoms on the surface of the monolayer are rather low and because the atoms lose their kinetic energy only very slowly they will move rather rapidly across the surface. Another possibility therefore is that the high lateral mobility may allow Pb atoms to coalesce, forming large three-dimensional clusters on the surface which will be very difficult to detect by x-ray photoemission spectroscopy or STM because of their low island density.

A possible objection to these arguments is that they do not apply to Bi. However, at this point the different bonding properties of Pb and Bi could be important. Bi has three $6p$ valence electrons, with three $pp\sigma$ bonds stabilizing a three-dimensional network (we shall not discuss here the structures of crystalline Bi). In contrast the two $6p$ electrons of Pb favor planar arrangements. Thus a Bi monolayer has free valencies for binding a second layer while a Pb monolayer has not. Of course all these arguments are speculative—a definite assessment will require extensive simulations of the adsorption process which are beyond the scope of the present work.

VII. SUMMARY AND CONCLUSIONS

We have studied the geometric and electronic structure of the quasiperiodic Pb monolayers grown on the fivefold *i*-Al-Pd-Mn surface. We have constructed structural models of the monolayer at two different coverages. The skeleton of the structure of the Pb monolayer consists of a network of the SF clusters. It may be described as a decorated P1 tiling and displays superstructure effects describable in terms of a τ-inflated τP1 tiling. The structural models reproduce all features seen in the experimental STM images, including the occurrence of bright spots located at the vertices of the τP1 tiling. The bright spots appear in the centers of the uP (or D) tiles where the substrate has Al atoms at these positions. The models also provide an explanation for the origin of the τ-scaled white flower motif observed in the STM.

The calculated electronic structure reveals that the density of states of the quasiperiodic monolayer exhibits a pseudogap at the Fermi level—in agreement with previous experimental observations. The comparison with electronic density of states of a freestanding quasiperiodic monolayer shows that the formation of this pseudogap cannot be attributed to the quasiperiodic arrangement of the Pb atoms but is induced by the hybridization of the Pb p states with the substrate.

ACKNOWLEDGMENTS

We acknowledge the European Network of Excellence on Complex Metallic Alloys (CMA) under Contract No. NMP3-CT-2005-500145, EPSRC under Grant No. EP/D05252X/1, and the Agence Nationale de la Recherche, Reference No. ANR-07-Blan-0270 for financial support. The work has been supported by the Austrian Ministry for Education, Science and Art through the Center for Computational Materials Science. M.K. thanks also for support from the Grant Agency for Science of Slovakia (Grant No. 2/5096/25) and from the Slovak Research and Development Agency (Grant No. APVV-0413-06, CEX-Nanosmart).

*Corresponding author; fyzikraj@savba.sk

[1] B. Bolliger, V. E. Dmitrienho, M. Erbudak, R. Lüscher, and H.-U. Nissen, Rev. B **63**, 052203 (2001).

[2] M. Shimoda, J. Q. Guo, T. J. Sato, and A. P. Tsai, Jpn. J. Appl. Phys. **40**, 6073 (2001).

[3] D. Naumović, P. Aebi, L. Schlapbach, C. Beeli, K. Kunze, T. A. Lograsso, and D. W. Delaney, Phys. Rev. Lett. **87**, 195506 (2001).

[4] K. J. Franke, H. R. Sharma, W. Theis, P. Gille, Ph. Ebert, and K. H. Rieder, Phys. Rev. Lett. **89**, 156104 (2002).

[5] V. Fournée, T. C. Cai, A. R. Ross, T. A. Lograsso, J. W. Evans, and P. A. Thiel, Phys. Rev. B **67**, 033406 (2003).

[6] T. Cai, J. Ledieu, R. McGrath, V. Fournée, T. Lograsso, A. Ross, and P. Thiel, Surf. Sci. **526**, 115 (2003).

[7] J. Ledieu, J. T. Hoeft, D. E. Reid, J. A. Smerdon, R. D. Diehl, T. A. Lograsso, A. R. Ross, and R. McGrath, Phys. Rev. Lett. **92**, 135507 (2004).

[8] H. R. Sharma, M. Shimoda, A. R. Ross, T. A. Lograsso, and A. P. Tsai, Phys. Rev. B **72**, 045428 (2005).

[9] H. R. Sharma, M. Shimoda, A. R. Ross, T. A. Lograsso, and A. P. Tsai, Philos. Mag. **86**, 807 (2006).

[10] A. K. Shukla, R. S. Dhaka, C. Biswas, S. Banik, S. R. Barman, K. Horn, Ph. Ebert, and K. Urban, Phys. Rev. B **73**, 054432 (2006).

[11] R. D. Diehl, N. Ferralis, K. Pussi, M. W. Cole, W. Setyawan, and S. Curtarolo, Philos. Mag. **86**, 863 (2006).

[12] B. Unal, V. Fournée, K. J. Schnitzenbaumer, C. Ghosh, C. J. Jenks, A. R. Ross, T. A. Lograsso, J. W. Evans, and P. A. Thiel, Phys. Rev. B **75**, 064205 (2007).

[13] J. A. Smerdon, J. K. Parle, L. H. Wearing, T. A. Lograsso, A. R. Ross, and R. McGrath, Phys. Rev. B **78**, 075407 (2008).

[14] J. Ledieu, L. Leung, L. H. Wearing, R. McGrath, T. A. Lograsso, D. Wu, and V. Fournée, Phys. Rev. B **77**, 073409 (2008).

[15] A. K. Shukla, R. S. Dhaka, S. W. D'Souza, S. Singh, D. Wu, T. A. Lograsso, M. Krajčí, J. Hafner, K. Horn, and S. R. Barman, Phys. Rev. B **79**, 134206 (2009).

[16] J. Ledieu, M. Krajčí, J. Hafner, L. Leung, L. H. Wearing, R. McGrath, T. A. Lograsso, D. Wu, and V. Fournée, Phys. Rev. B **79**, 165430 (2009).

[17] M. Krajčí and J. Hafner, Phys. Rev. B **71**, 184207 (2005).

[18] M. Krajčí and J. Hafner, Phys. Rev. B **75**, 224205 (2007).

[19] M. Krajčí and J. Hafner, Phys. Rev. B **77**, 134202 (2008).

[20] M. Krajčí and J. Hafner, Phys. Rev. B **71**, 054202 (2005).

[21] M. Krajčí, J. Hafner, J. Ledieu, and R. McGrath, Phys. Rev. B **73**, 024202 (2006).

[22] Z. Papadopolos, G. Kasner, J. Ledieu, E. J. Cox, N. V. Richardson, Q. Chen, R. D. Diehl, T. A. Lograsso, A. R. Ross, and R. McGrath, Phys. Rev. B **66**, 184207 (2002).

[23] G. Kasner and Z. Papadopolos, Philos. Mag. **86**, 813 (2006).

[24] T. M. Schaub, D. E. Bürgler, H.-J. Güntherodt, and J.-B. Suck, Phys. Rev. Lett. **73**, 1255 (1994).

[25] J. Ledieu and R. McGrath, J. Phys.: Condens. Matter **15**, S3113 (2003).

[26] Z. Papadopolos, P. Pleasants, G. Kasner, V. Fournée, C. J. Jenks, J. Ledieu, and R. McGrath, Phys. Rev. B **69**, 224201 (2004).

[27] G. Kresse and J. Furthmüller, Comput. Mater. Sci. **6**, 15 (1996); Phys. Rev. B **54**, 11169 (1996).

[28] G. Kresse and D. Joubert, Phys. Rev. B **59**, 1758 (1999).

[29] M. Boudard, M. de Boissieu, C. Janot, G. Heger, C. Beeli, H.-U. Nissen, H. Vincent, R. Ibberson, M. Audier, and J. M. Dubois, J. Phys.: Condens. Matter **4**, 10149 (1992).

[30] M. Krajčí, M. Windisch, J. Hafner, G. Kresse, and M. Mihalkovič, Phys. Rev. B **51**, 17355 (1995).

[31] B. Unal, C. J. Jenks, and P. A. Thiel, Phys. Rev. B **77**, 195419 (2008).

[32] M. Krajčí, J. Hafner, J. Ledieu, and V. Fournée, J. Phys.: Conf. Ser. **226**, 012005 (2010).

[33] N. E. Christensen, S. Satpathy, and Z. Pawlowska, Phys. Rev. B **34**, 5977 (1986).

[34] W. Jank and J. Hafner, Phys. Rev. B **41**, 1497 (1990).

[35] T. Fujiwara, Phys. Rev. B **40**, 942 (1989).

[36] J. Hafner and M. Krajčí, Phys. Rev. Lett. **68**, 2321 (1992).

[37] J. Hafner and M. Krajčí, Phys. Rev. B **47**, 11795 (1993).

[38] Z. M. Stadnik, D. Purdie, M. Garnier, Y. Baer, A.-P. Tsai, A. Inoue, K. Edagawa, S. Takeuchi, and K. H. J. Buschow, Phys. Rev. B **55**, 10938 (1997).

[39] M. Krajčí and J. Hafner, J. Phys.: Condens. Matter **12**, 5831 (2000).

[40] M. Krajčí and J. Hafner, J. Phys.: Condens. Matter **14**, 5755 (2002).

[41] R. Asahi, H. Sato, T. Takeuchi, and U. Mizutani, Phys. Rev. B **72**, 125102 (2005).

[42] E. S. Zijlstra and T. Janssen, Phys. Rev. B **61**, 3377 (2000).

[43] Z. M. Stadnik, D. Purdie, Y. Baer, and T. A. Lograsso, Phys. Rev. B **64**, 214202 (2001).

[44] E. S. Zijlstra and S. K. Bose, Phys. Rev. B **67**, 224204 (2003).

[45] R. Widmer, P. Gröning, M. Feuerbacher, and O. Gröning, Phys. Rev. B **79**, 104202 (2009).

[46] J. Hafner and W. Jank, Phys. Rev. B **45**, 2739 (1992).

[47] J. B. Suck, in *Quasicrystals*, edited by J. B. Suck, M. Schreiber, and P. Häussler (Springer, Berlin, 2002), p. 467.

[48] B. N. Brockhouse T. Arase, G. Cagliotti, K. R. Rao, and A. D. B Woods, Phys. Rev. **128**, 1099 (1962).